Effects of Purified Recombinant Neural and Muscle Agrin on Skeletal Muscle Fibers In Vivo

Gabriela Bezakova,* Johannes P. Helm,‡ Maura Francolini,§ and Terje Lømo*

*Department of Physiology and ‡Department of Anatomy, University of Oslo, 0317 Oslo, Norway; and §C.N.R. Center for Cellular and Molecular Pharmacology, Department of Medical Pharmacology, University of Milano, 20129 Milan, Italy

Abstract. Aggregation of acetylcholine receptors (AChRs) in muscle fibers by nerve-derived agrin plays a key role in the formation of neuromuscular junctions. So far, the effects of agrin on muscle fibers have been studied in culture systems, transgenic animals, and in animals injected with agrin–cDNA constructs. We have applied purified recombinant chick neural and muscle agrin to rat soleus muscle in vivo and obtained the following results. Both neural and muscle agrin bind uniformly to the surface of innervated and denervated muscle fibers along their entire length. Neural agrin causes a dose-dependent appearance of AChR aggregates, which persist ≥7 wk after a single application. Muscle agrin does not cluster AChRs and at 10 times the concentration of neural agrin does not reduce binding or AChR-aggregating activity of neural agrin. Electrical muscle activity affects the stability of agrin binding and the number, size, and spatial distribution of the neural agrin–induced AChR aggregates. Injected agrin is recovered from the muscles together with laminin and both proteins coimmunoprecipitate, indicating that agrin binds to laminin in vivo. Thus, the present approach provides a novel, simple, and efficient method for studying the effects of agrin on muscle under controlled conditions in vivo.

Key words: agrin • acetylcholine receptors • laminin • electrical activity • neuromuscular junction

Introduction

Signaling between nerve and muscle occurs at neuromuscular junctions (NMJs)[1], which consist of specialized and precisely apposed pre- and postsynaptic structures separated by a synaptic cleft (Sanes and Lichtman, 1999). Agrin, a heparan sulfate proteoglycan of ∼400–600 kD, is essential for the induction and organization of the postsynaptic structures (McMahan, 1990; Gautam et al., 1996; Cohen et al., 1997; Jones et al., 1997; Meier et al., 1997; Rimer et al., 1997). Agrin is synthesized by motor neurons, transported to axon terminals, and released into the synaptic cleft of NMJs, where it binds to the basal lamina (Magill-Solc and McMahan, 1988, 1990; Cohen and Godfrey, 1992; Reist et al., 1992). Motor neurons express a mixture of agrin isoforms, alternatively spliced at two sites (A and B in chick, y and z in rat) in their COOH-terminal halves (Ruegg et al., 1992; Rupp et al., 1992; Hoch et al., 1993). The neural isoform of agrin containing inserts of four and eight amino acids at sites A and B, respectively, is most effective in clustering acetylcholine receptors (AChRs) in vitro (Gesemann et al., 1995). Muscle cells and other nonneuronal cells also express agrin, but as isoforms that lack inserts at sites A and B and fail to cluster AChRs (Ruegg et al., 1992; Hoch et al., 1993; Ma et al., 1994; Smith and O'Dowd, 1994).

The AChR-clustering activity of neural agrin has been well characterized in vitro, where the activity is both concentration- and Ca^{2+}-dependent (Nastuk et al., 1991; Gesemann et al., 1996; Megeath and Fallon, 1998). When bound to extracellular matrix, neural agrin increases the transcription of AChR ε-subunits in addition to clustering AChRs (Jones et al., 1996). Biochemical and immunological studies show that agrin binds in a Ca^{2+}-dependent manner to α-dystroglycan, a component of the dystrophin-associated glycoprotein complex present on the surface of muscle fibers (Gee et al., 1994), as well as to laminin in the basal lamina (Denzer et al., 1997; Kammerer et al., 1999). However, the physiological consequences of these bindings are not clear. Other proteins have been implicated to interact with agrin in vitro but none of them has been shown to be critical for postsynaptic differentiation in vivo (Sanes et al., 1998).

The most compelling evidence that agrin is essential for NMJ formation comes from loss- and gain-of-function

---

Address correspondence to Gabriela Bezakova, Department of Pharmacology/Neurobiology, Biozentrum, University of Basel, Klingelbergstrasse 50, CH-4056 Basel, Switzerland. Tel.: 41-61-267-2214. Fax: 41-61-267-2208. E-mail: gabriela.bezakova@unibas.ch

[1]*Abbreviations used in this paper:* AChR, acetylcholine receptor; EB, extraction buffer; Fl-BuTx, FITC-bungarotoxin; NMJ, neuromuscular junction; PFA, paraformaldehyde; Rh-BuTx, TRITC-α-bungarotoxin; SOL, soleus.

studies. In agrin-deficient mutant mice, the postsynaptic differentiation was profoundly impaired and the mice died perinatally (Gautam et al., 1996). A similar phenotype was observed in mutant mice lacking muscle specific kinase (MuSK), a transmembrane protein tyrosine kinase selectively expressed at the NMJ in innervated skeletal muscle (Valenzuela et al., 1995; DeChiara et al., 1996), making it a good candidate for the agrin receptor. However, the physical interaction between agrin and MuSK has not yet been identified. Instead, MuSK and other proteins have been suggested to create a multisubunit agrin receptor complex (Glass et al., 1996).

Experiments involving implantation of agrin-secreting myoblasts or injection of agrin expression constructs into muscles demonstrated agrin's activity in vivo (Cohen et al., 1997; Jones et al., 1997; Meier et al., 1997; Rimer et al., 1997). Expression of neural agrin in transfected cells followed by its release and deposition on neighboring fibers induced multiple AChR aggregates. When expressed in electrically active muscles, the ectopic AChR aggregates acquired features typical for adult NMJ, having junctional folds and functional electrophysiological properties (Meier et al., 1997). Thus, agrin alone appears capable of assembling a fully functional postsynaptic apparatus.

Formation of ectopic NMJs through the interaction of transplanted axons with soleus (SOL) muscles is strongly affected by electrical muscle activity (Lømo and Slater, 1978; Brenner et al., 1987; Rotzler and Brenner, 1990; Skorpen et al., 1999). Neural agrin induces ectopic postsynaptic-like apparatuses in SOL muscles that are similarly affected by electrical activity (Mathiesen et al., 1999). Hence, these experimental models allowed the comparison the formation of nerve- and agrin-induced NMJs in vivo under the most physiological conditions examined so far.

Injecting agrin–cDNA into muscles is a useful in vivo approach, which nonetheless has drawbacks because it is difficult to transfect more than a few fibers in each muscle and to determine the dose and site of agrin release. Here, we present the results of a different approach based on in vivo applications of known concentrations of purified recombinant neural and muscle chick agrin. We use this approach to study properties of neural and muscle agrin with regard to their binding to the surface of muscle fibers, AChR-aggregating activity, and modulation by electrical muscle stimulation. We find that a single injection of neural agrin induces ectopic AChR aggregates along muscle fibers, which are dose dependent and persist ≥7 wk. After injection, neural agrin binds to laminin and uniformly to the surface of muscle fibers along their entire length. Subsequently, the amount of bound neural agrin and the distribution and appearance of neural agrin–induced AChR aggregates are regulated by electrical muscle activity. Muscle agrin displays similar binding but fails to aggregate AChRs.

Materials and Methods

Purification of Recombinant Agrin

Recombinant full-length chick neural and muscle agrin were purified from the conditioned media of stably transfected HEK 293 cells (gift of Dr. M.A. Ruegg, University of Basel, Basel, Switzerland) by modified method (Denzer et al., 1997). The cells were cultured in a DME supplemented with 10% FBS (BioWhittaker) until they became confluent. FBS-free DME medium was then used for 5–7 d. The conditioned medium was collected, and the protein was purified by a batch technique using mono Q Sepharose beads (Amersham Pharmacia Biotech). After rotating at 4°C overnight, the beads were washed on the column with 20 mM Tris-HCl, pH 7.2, 0.5 M NaCl. Bound proteins were eluted with 2 M NaCl, and 1 ml fractions were collected. Protein-containing fractions were further analyzed by SDS-PAGE (Laemmli, 1970) on a 3–12% gradient gel and visualized by Coomassie blue and silver stainings. Agrin-containing fractions were dialyzed against PBS, pH 7.4. Protein concentration was determined by Bradford protein assay (Bio-Rad Laboratories), using BSA as a standard.

Metabolic Labeling of Agrin

Confluent cultures, as described above, were switched to 25% DME and 75% DME without methionine and cysteine supplemented with Tran Sulfur-35 label (20 μCi/ml; ICN Biomedicals). The purified proteins were separated by SDS-PAGE on 3–12% gradient gels. Gels were dried and exposed to the film (Eastman Kodak Co.).

Surgical Procedures and In Vivo Stimulation

The experiments were carried out on adult male Wistar rats (∼250 g body weight). All surgical procedures were done under general anesthesia by Equithesin (0.4 ml/100 g body weight) injected i.p. SOL muscles were denervated by removing ∼5 mm of the sciatic nerve in the thigh. For stimulation, uninsulated ends of two wires (AS 632, Cooner) were placed across the muscle, run under the skin through an attachment by screws, dental cement to the skull, and a flexible plastic tube to rotating contacts ∼0.5 m above the rat (Windisch et al., 1998). Stimulation started 1 h later and consisted of 60 0.4-ms bipolar square pulses at 100 Hz every 60 s for ≤9 d. Identical experiments have been inspected and approved by the Norwegian Experimental Board and Ethical Committee for Animal Experiments on several occasions. The present experiments were overseen by the veterinarian responsible for the animal house. The animals were checked daily. The flexible tube overhead allowed free movements within the cage. Apart from one leg being denervated and contractions being visible during stimulation, the animals did not show obvious abnormal behavior or signs of pain.

Application of Recombinant Agrin

Intramuscular Injection. SOL muscles were injected intramuscularly with 70 μl of 1 μM recombinant chick neural or muscle agrin. The sciatic nerve was either cut immediately thereafter or kept intact. The muscle was excised at different time points, labeled with TRITC-α-bungarotoxin (Rh-BuTx; Molecular Probes) for 30 min, washed with PBS, and fixed with 1.5% paraformaldehyde (PFA). Fixed muscle was teased into ∼30 thin bundles containing 50–100 muscle fibers. Bundles showing signs of damage were few, attributed to the injection or overlying electrodes, and excluded from analysis. We did not observe morphological changes or mononucleated cells indicative of significant immune response.

Bathing of SOL Muscle with Agrin. To study the effects of different concentrations of agrin, SOL was exposed in situ and carefully dissected free from surrounding tissue except at tendons and entries of nerve and blood vessels. Under deep anesthesia, SOL was then bathed for 2 h in PBS alone or PBS containing from 100 pM–10 μM agrin. Fresh solution was repeatedly added to the bath to keep the SOL fully immersed. After 2 h, the opening in the leg was rinsed with PBS and closed with sutures through overlying muscles, fascias, and skin. The muscles were excised 4 or 7 d later, labeled with Rh-BuTx, washed with PBS, and fixed with 1.5% PFA. 4 d were chosen for denervated fibers because at 4 d obvious reorganization of the AChR aggregates had not yet occurred and the aggregates were still uniformly distributed along fibers (see Fig. 2). 7 d were chosen for innervated fibers because comparable reorganization of AChR aggregates did not occur on innervated fibers and staining was stronger after 7 than 4 d (see Fig. 2). At 4 or 7 d, a thin layer of surface fibers, which had been in direct contact with the agrin solution, was dissected out and examined with an Olympus AX70 fluorescence microscope. Images were captured with a Colour Coolview charge-coupled device camera (Photonic Science).

Quantification of AChR-aggregating Activity

Relative Area Occupied by AChR Aggregates. Agrin-induced AChR aggregates that could be viewed en face on the surface of single muscle fiber at 1,000× magnification were selected for measurements using an Open Lab imaging software (Improvision). A rectangular region enclosing a collec-

tion of these aggregates was drawn, and the areas of all the individual aggregates within the region were measured and summed. The sum of such areas was expressed as a percentage of the rectangular region and taken as a measure of agrin AChR-aggregating activity. Collections of AChR aggregates on differently treated muscle fibers were summed within the rectangle of the same size.

Intensity of Fluorescent Labeling. The imaging system was calibrated, using the InSpeck Microscope Image Intensity Calibration Kit (Molecular Probes) containing microspheres coated with six different concentrations of fluorescent dye. To obtain the specific mean labeling intensity of aggregates, the mean intensity of an adjacent aggregate-free part of the fiber (background) was subtracted from the mean intensity of the aggregates (Turney et al., 1996). The subtracted value was then normalized by the value given by microspheres coated with 3% of fluorescent dye obtained in the same session. 20 images in each of 3 similarly treated muscles were analyzed in randomly chosen extrajunctional regions of denervated fibers and in regions near the myotendinous junctions of innervated fibers, where most of the aggregates were located (see Fig. 3 A).

Immunocytochemistry

Teased muscle bundles were labeled with Rh-BuTx for 30 min, washed with PBS, and fixed in 1.5% PFA. The labeling of ε- and γ-subunits was performed as described by Missias et al. (1996) and Gu et al. (1991), respectively (gift of Dr. J. Sanes, Washington University, St. Louis, MO). The primary antibodies were visualized by FITC-conjugated anti–rabbit secondary antibodies (Sigma-Aldrich) at dilution 1:200. The samples were observed with a confocal laser-scanning microscope (TCS-SP; Leica) equipped with an Ar^+ Kr^+ ion laser. Excitation was done at 488 and 568 nm, and the spectrometer settings (width and positions of the slits in front of the photomultiplier tubes) were selected in order to minimize cross-bleeding between the FITC and the TRITC channels.

Autoradiography of Muscle Fibers from Muscles Injected with ^{35}S-labeled Agrin

SOL muscles were injected with 70 μl of 1 μM ^{35}S-labeled neural or muscle agrin. The muscles were excised 1 and 4 d later and fixed with 2.5% glutaraldehyde overnight. Single muscle fibers were teased out and placed on gelatine-coated slides. The muscle fibers were covered with a film emulsion (Eastman Kodak Co.), as previously described (Salpeter and Azabo, 1976). The film was developed after appropriate time and the amount and distribution of silver grains were analyzed using a confocal laser-scanning microscope (TCS-SP; Leica) equipped with an Ar^+ Kr^+ ion laser. The specimens were scanned using a Plan Apochromat 63 × 1.32 oil immersion lens. The scans were done in the reflection mode. When examining the specificity of ^{35}S-labeled agrin binding, the muscle was injected with 70 μl of 10 μM unlabeled agrin isoform 6 h before injection of the same volume of 1 μM labeled agrin isoform. Similar studies were performed using combination of muscle and neural agrin. Fibers teased from muscle injected with PBS were used to control for unspecific background. 10 fibers teased at random from each of 3 similarly treated muscles were placed on glass slides such that each slide contained fibers for each experimental condition and control. In this way, only fibers undergoing identical processing were compared.

Identification of Agrin Binding to Laminin

Sequential Protein Extraction. 1 d after the injection of recombinant neural or muscle ^{35}S-labeled agrin, the muscles were dissected out and frozen in liquid nitrogen. The tissues were then homogenized in 10 vol (wt/vol) of ice-cold homogenization buffer containing 10 mM Na phosphate, pH 7.4, 150 mM NaCl, 5 mM EDTA plus a cocktail of protease inhibitors (aprotinin, leupeptin, benzamidin, pepstatin at 0.5 μg/ml each and 2 mM PMSF) using a polytron. The homogenate was centrifuged for 20 min at 12,000 g. The supernatant was collected (PBS-EDTA fraction), and the pellet was further extracted with homogenization buffer plus 1% Triton X-100 (extraction buffer [EB]) using Dounce homogenizer. The extract was centrifuged 20 min at 50,000 g. The supernatant was separated (Triton X-100 fraction), and the pellet was boiled for 10 min with gel denaturing or nondenaturing loading buffers (pellet fraction). Individual fractions were separated on 3–12% gradient gels using denaturing and reducing or nondenaturing nonreducing conditions. The gels were dried and exposed to the film (Eastman Kodak Co.). The position and the size of radioactively labeled bands were analyzed.

Immunoprecipitation and Western Blot. SOL muscle was dissected from rats previously injected with recombinant neural or muscle agrin and frozen in liquid nitrogen. The tissue was then extracted in 10 vol (wt/vol) of ice-cold EB using a Polytron. The homogenate was centrifuged for 20 min at 50,000 g. The supernatant was collected and incubated with mAb 5B1 overnight at 4°C. Protein A–agarose (Sigma-Aldrich) was added for 4 h at 4°C. The beads were then applied on a column and washed with 50 vol of EB. Bound proteins were eluted with SDS sample buffer. The eluted fraction was separated on 3–12% SDS-PAGE gel. Proteins were either visualized by silver staining or transferred to nitrocellulose membrane using standard methods (Towbin et al., 1979). After blocking, the membranes were incubated overnight with polyclonal antibody against α2-laminin diluted 1:5,000 (gift of Dr. R. Timpl, Max-Plank Institute, Martinstried, Germany). The primary antibody was detected with appropriate secondary antibody conjugated to HRP (Jackson ImmunoResearch Laboratories) diluted 1:2,000. Bands were visualized by chemiluniscence (Pierce Chemical Co.) and exposed to the film (Eastman Kodak Co.).

Results

Purification of Full-Length Chick Neural and Muscle Agrin

Full-length chick neural and muscle recombinant agrin (Fig. 1 A) was purified from cultures of stably transfected 293 HEK cells using an ion exchange chromatography as described in Materials and Methods. Both proteins appeared on 3–12% SDS-PAGE gradient gels stained with Coomassie blue or silver as single smeared bands with an apparent molecular weight of 400–600 kD (Fig. 1, B and C). Comparable bands were observed after immunoprecipitation with mAb 5B1 (Reist et al., 1987) or a polyclonal antiserum against chick agrin polyclonal antibody 3228 (Gesemann et al., 1995), confirming the identity of the proteins (Fig. 1 D).

Fate of AChR Aggregates after a Single Injection of Neural Agrin

A single injection of purified recombinant neural agrin (1 μM, 70 μl) into innervated or denervated SOL muscles in vivo caused aggregation of AChRs on the surface of muscle fibers outside the original NMJs (Fig. 2 A). Without such injections, AChR aggregates were not observed. In both muscles, AChR aggregates had already formed on day 3, the earliest time point examined. In muscles denervated at the time of injection, the aggregates were initially numerous, small (∼4 μm), punctate, and uniformly distributed along the fibers. During the next 1–2 wk, they became larger and surrounded by regions with reduced number of aggregates. These larger aggregates persisted ≥7 wk after the injection, the latest time point examined. They were formed, most probably, by coalescence of smaller clusters since aggregates labeled by injection of Rh-BuTx on day 7 had become similarly reorganized when examined 14 d later (Fig. 2 B). In addition, the colocalization of aggregates labeled by Rh-BuTx on day 7 and by FITC-bungarotoxin (Fl-BuTx) on day 21 shows that the aggregates became structurally stable with newly synthesized AChRs (labeled on day 21) inserted at aggregates containing old AChRs (labeled on day 7). No AChR aggregates appeared in a 0.5–0.8-mm-long region on each side of the NMJ, except for a few punctate clusters in the immediate vicinity of the junction (Fig. 3 B).

The AChR aggregates induced on innervated muscles were different. They were much fewer in number, larger, more uniform in size (mean length ∼130 μm), structurally
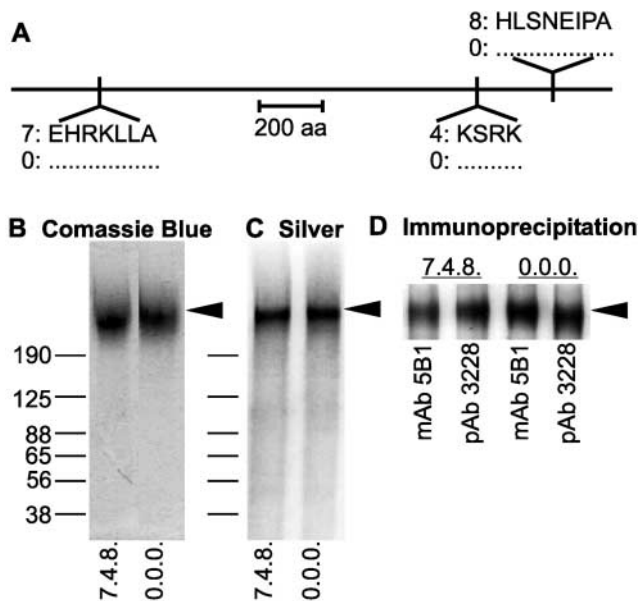
Figure 1. Characterization of full-length chick neural and muscle agrin purified from stably transfected 293 HEK cells. (A) Location of alternatively spliced sites characteristic for neural (7.4.8.) and nonneural or muscle (0.0.0.) agrin isoforms together with their amino acid sequences. The fractions of purified agrin collected by ion exchange chromatography contained high concentrations of agrin that were easily detectable by Comassie blue staining (B) and were >90% pure as shown by Silver staining (C). Immunoprecipitation (D) using the mAb against agrin (mAb 5B1) or antiagrin antiserum (polyclonal antibody 3228) confirmed that the purified protein is chick agrin. Proteins were separated by 3–12% SDS-PAGE. Molecular masses of standard proteins are indicated in kD in B. Arrows point to the smeared bands of purified neural and muscle agrin with the apparent molecular of 400–600 kD.

Figure 2. Ectopic AChR aggregates induced by purified recombinant chick neural agrin. (A) A single injection of 1 μM agrin into acutely denervated (left) or innervated (right) SOL muscles caused the appearance of numerous AChR aggregates at the indicated times after injection. Note differences in number, size, and distribution of aggregates labeled with Rh-BuTx in denervated and innervated muscles. In innervated muscles, the aggregates appeared predominantly near myotendinous junctions (see also Fig. 3). (B) SOL muscle was injected with agrin and denervated on day 0. On day 7, it was injected with Rh-BuTx, removed, and labeled with Fl-BuTx on day 21. Presence of Rh-BuTx–labeled aggregates on day 21 shows their metabolic stability; colocalization of Rh-BuTx and Fl-BuTx indicates the structural stability of aggregates.

stable, and preferentially located near the myotendinous junction (Fig. 3 A), where the aggregates illustrated in Fig. 2 A were formed. Also in this case, the perisynaptic region on each side of the original NMJs was devoid of AChR aggregates, except for those in the immediate vicinity of the junction (Fig. 3 C).

The phenomena just described were neither species nor muscle type specific since SOL and EDL in both rat and mouse responded similarly (data not shown).

AChR-aggregating Activity of Neural Agrin: Dependence on Dose and Innervation

To examine the influence of innervation on neural agrin's AChR-aggregating activity, we compared the effects of different concentrations of neural agrin on predenervated (7 d), acutely denervated, and innervated SOL muscles. In these experiments, we applied neural agrin at different concentrations to the exposed surface of SOL muscles for 2 h and examined the surface fibers for AChR aggregates after 4 (denervated muscles) or 7 (innervated muscles) d (see Materials and Methods). Predenervated and acutely denervated muscles responded similarly (Fig. 4). With increasing agrin concentration, individual AChR aggregates became first larger and then smaller in size. In innervated
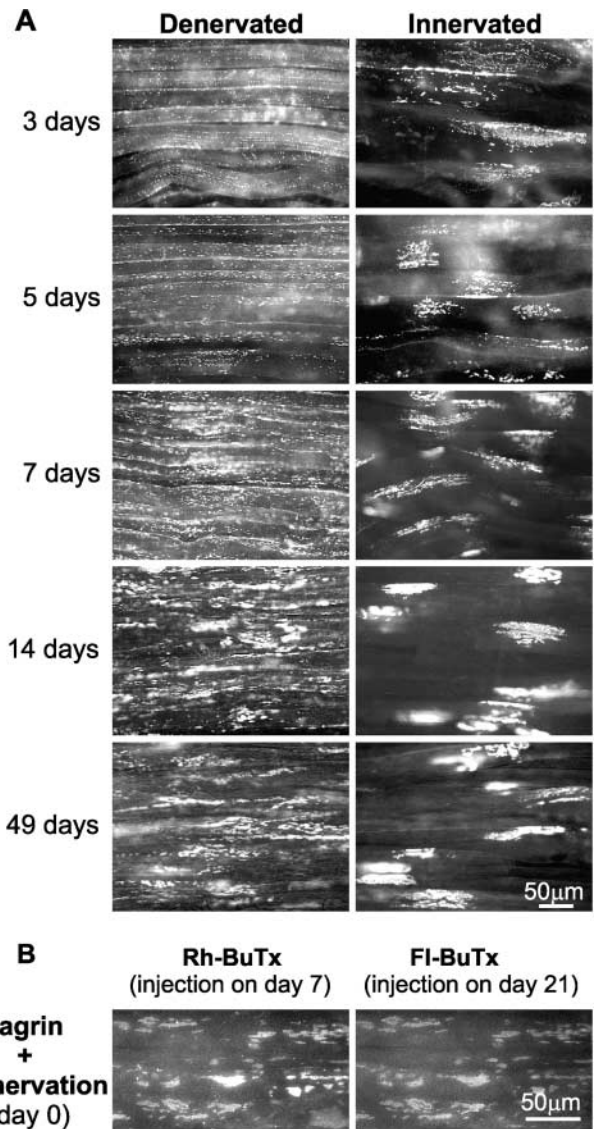
fibers, similar profile of responses was observed but the threshold concentration for induction of AChR aggregates was 100-fold higher (Fig. 4).

These results are shown quantitatively in Fig. 5 and Table I. There was no major difference in EC_{50} (agrin concentration necessary to induce half-maximal response) between predenervated and acutely denervated muscles, except that the area occupied by AChR aggregates for a given area of fiber surface became moderately larger in the predener-
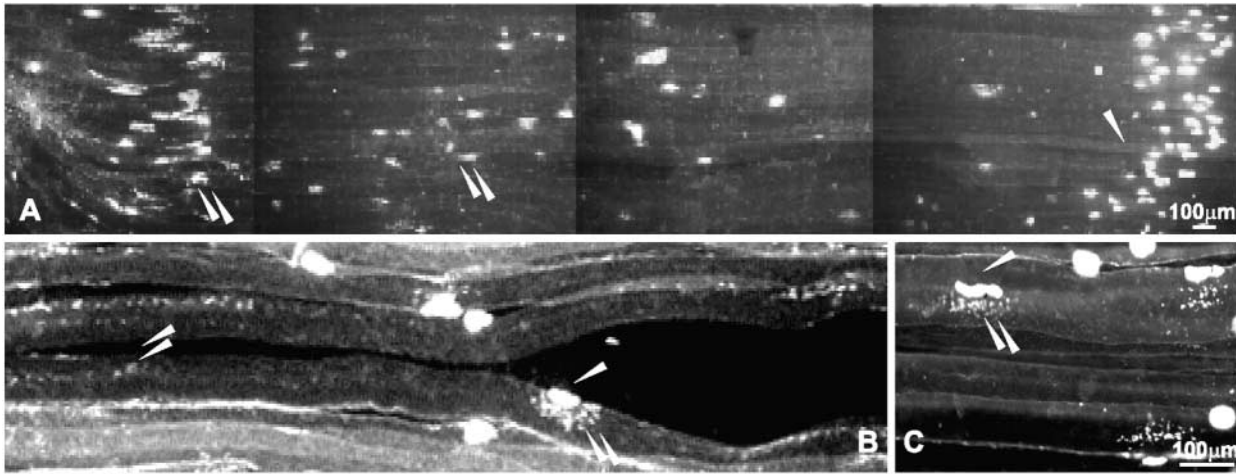
Figure 3. Distribution of AChR aggregates induced by injection of 1 μM neural agrin into innervated (A and C) or denervated (B) muscles. In innervated muscles, most of the aggregates appeared near myotendinous junction (to the left in A). In denervated muscles, AChR aggregates were essentially absent near the original NMJs (B) but abundant elsewhere (see also Fig. 2). Small punctate aggregates appeared in the area immediately adjacent to the original NMJs in both innervated and denervated muscles (B and C). The large majority of agrin-induced aggregates were distinguished from the original NMJs by their different appearance, location outside the characteristic band of NMJs across the middle of the muscle, and weaker intensity of Rh-BuTx staining. The few punctate aggregates close to the NMJs were distinguished by their appearance since nothing like them was observed near innervated or denervated NMJs without injecting neural agrin. Double arrow points to agrin-induced ectopic AChR aggregates; single arrow points to original NMJ.

vated muscles. On the other hand, the EC_{50} for the response of innervated muscles to neural agrin was 10 times higher.

The intensity of Rh-BuTx labeling (see Materials and Methods) increased with increasing agrin concentrations, also at the highest concentrations when individual aggregates became smaller and occupied a smaller area of the muscle fiber surface (Figs. 4 and 5 B, Table I). Furthermore, there was no significant difference between EC_{50} for
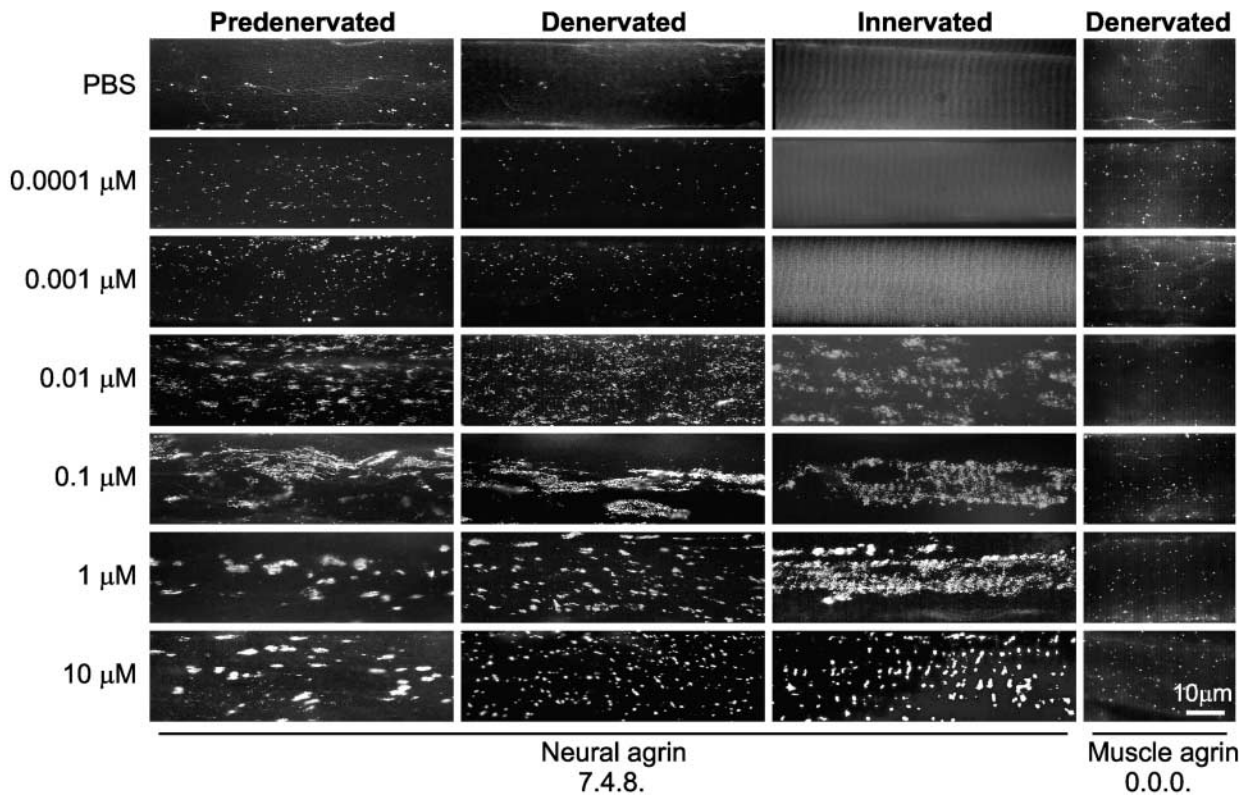

Figure 4. AChR-aggregating activity of neural agrin is dose dependent. 7-d denervated (predenervated), acutely denervated, or innervated SOL muscles were bathed in the solution of neural or muscle agrin at concentrations as indicated in vivo for 2 h. The muscles were dissected out after 4 (predenervated and acutely denervated) or 7 (innervated) d and labeled with Rh-BuTx. Only neural agrin induced AChR aggregates whose appearance was dependent on the dose applied.
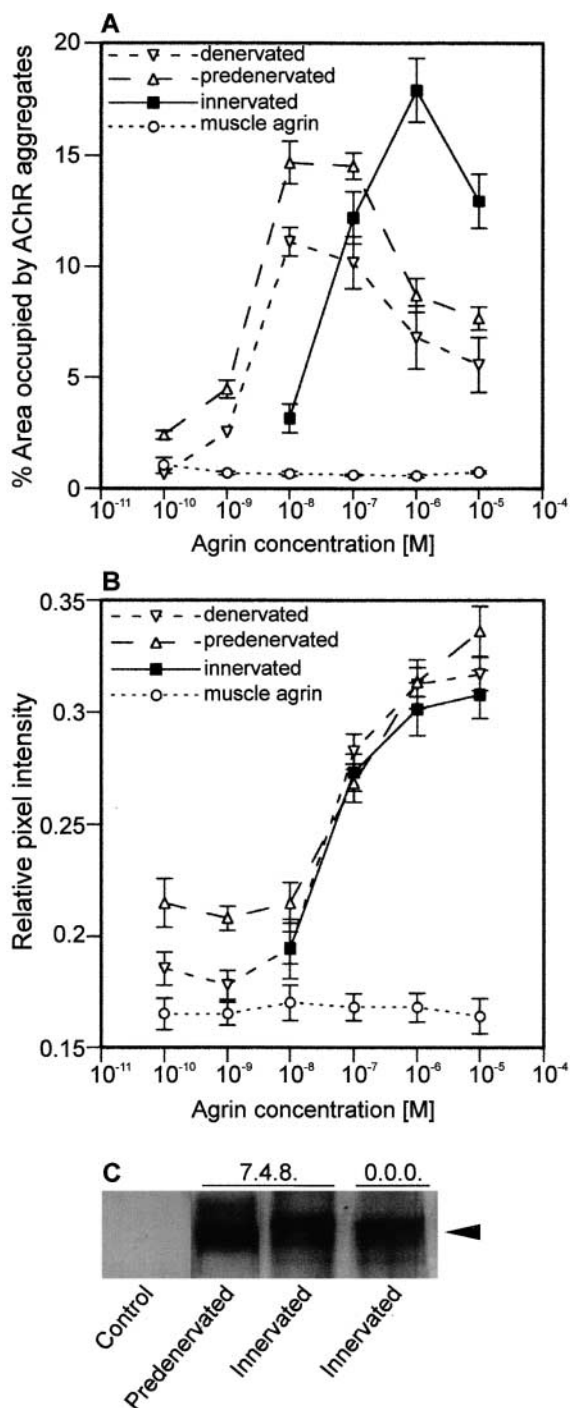
Figure 5. Dose-response curves from experiments illustrated in Fig. 4. The area of AChR aggregates as percentage of a given area of muscle fiber surface (A) and the relative fluorescence of the Rh-BuTx that labeled the aggregates (B) are plotted against concentration of applied agrin (see Materials and Methods). Plots represent mean values ± SEM of 20 collections of aggregates in each of three experiments for each concentration. Amount of neural and muscle agrin bound to the muscle was determined by immunoprecipitation 12 h after application (C).

(Figs. 4 and 5). To examine if these differences could be related to the switch from γ- to ε-subunit–containing AChRs that normally occurs at developing NMJs, we labeled the aggregates with antibodies specific for γ- and ε-subunits. In denervated muscles, little or no ε-subunit expression could be detected at any concentration. In contrast, in innervated muscles, the aggregates contained ε-subunits and little or no detectable γ-subunits (Fig. 6). Thus, the decline in size and the increase in labeling intensity observed at aggregates induced by the highest concentrations of agrin were not related to the content of γ- or ε-subunits in the aggregates.

Muscle agrin did not aggregate AChRs at any concentration (Figs. 4 and 5), even though muscle agrin bound well to the muscle surface (see below). Immunoprecipitation of injected neural and muscle chick agrin by species-specific mAbs followed by SDS-PAGE gels revealed bands of appropriate size and similar intensities (Fig. 5 C).

Electrical Muscle Stimulation Alters the Number, Size, and Distribution of AChR Aggregates Induced by Neural Agrin

The distribution and appearance of AChR aggregates induced by injected recombinant neural agrin were different in innervated and denervated muscles (Fig. 2 A). To examine if lack of electrical muscle activity could account for these differences, we started muscle stimulation 7 d after the muscle had been denervated and injected with neural agrin. Stimulation for 7 d removed most of the aggregates and caused those that survived to become similar in appearance and distribution to those observed in innervated muscles (Fig. 7, a and b). Accordingly, electrical muscle activity appears to be a major factor in controlling the distribution and organization of neural agrin–induced AChR aggregates.

To examine whether the number of AChR aggregates induced in the innervated muscle after a single injection could be increased by delayed denervation, we injected neural agrin into innervated muscles and then denervated the muscles for 7 d at different times afterwards. In muscles denervated 3 d after the injection (Fig. 7 f), multiple small AChR aggregates appeared that were indistinguishable from those induced by injecting neural agrin into denervated muscles (Fig. 7 d). A few larger aggregates were also observed, primarily near myotendinous junctions, which probably represented the aggregates induced in the muscle before the denervation. In muscles denervated 28 d after the injection, additional AChR aggregates still appeared but in smaller number (Fig. 7 j, compare with non-denervated fibers in c, e, g, and i). These results suggest that the amount of agrin initially bound along the muscle

half maximal labeling intensity in predenervated, denervated, and innervated muscles (Table I).

The size and organization of AChR aggregates depended strongly on the concentration of neural agrin
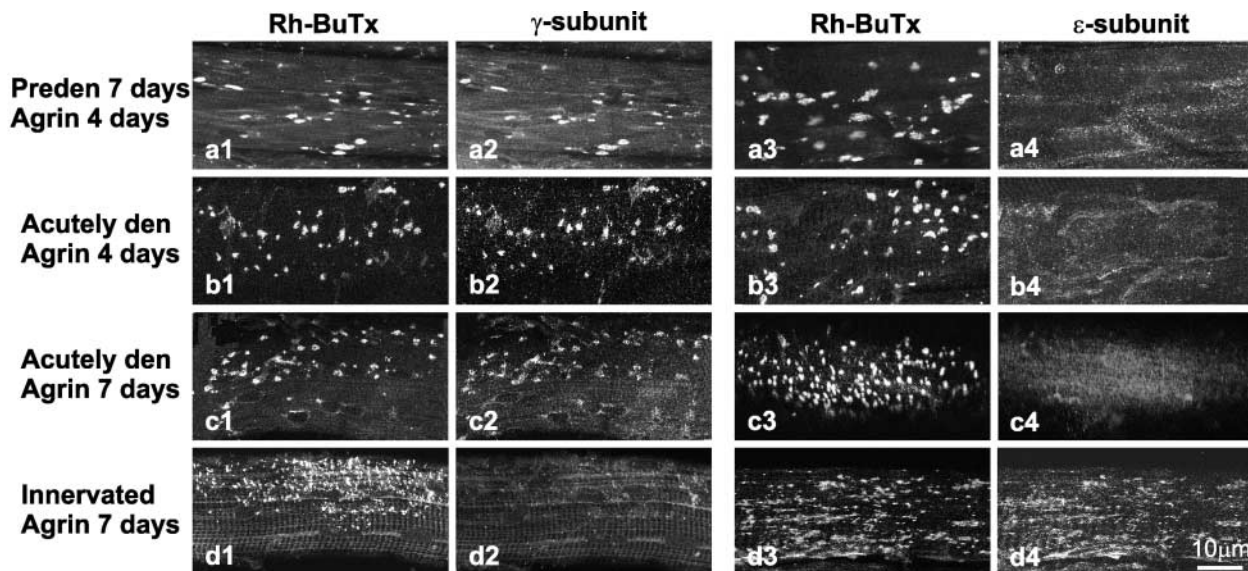
Figure 6. Presence of γ- and ε- AChR subunits in AChR aggregates induced by neural agrin. SOL muscles that were 7-d denervated (a), acutely denervated (b and c), or innervated (d) were bathed in PBS containing 10 μM neural agrin in vivo for 2 h. 4 (a and b) and 7 (c and d) d later, the muscles were excised and examined for AChR aggregates on surface fibers after labeling with Rh-BuTx and antibodies against γ- and ε-subunits, as indicated. Note that AChR aggregates on denervated fibers contained γ-subunits (a2, b2, and c2) and no detectable ε-subunits (a4, b4, and c4), whereas innervated fibers contained ε-subunits (d4) but little or no detectable γ-subunits (d2).

fiber of the innervated muscles was gradually decreasing. 4 wk after application, agrin was, however, still detectable by immunocytochemistry at the ectopic aggregates in the innervated muscles (not shown).

Distribution of Injected Agrin along Muscle Fibers

The AChR aggregates induced by neural agrin were discontinuous along the fibers. To determine whether this distribution corresponds to the distribution of injected agrin after binding onto the muscle fiber, we metabolically labeled neural and muscle agrin by [^{35}S]methionine and [^{35}S]cysteine using stably transformed 293 HEK cells (Fig. 8 A; see Materials and Methods). 1 d after injection, ^{35}S-labeled neural or muscle agrin, respectively, were detected by autoradiography at similar densities along the fibers (Fig. 8 B, a and b) of innervated muscle. 4 d after the injection, however, the density was much lower in innervated than in denervated fibers (Fig. 8 B, c–f). Moreover, many fibers contained in their midregion a site of higher grain density, which presumably corresponded to the original NMJs (Fig. 8, a and b, arrow). In agreement with this finding, we also detected recombinant chick agrin by immunocytochemistry at NMJs (not shown). We did not detect any gaps in the distribution of bound agrin in 1-d innervated or 4-d denervated muscles that could correspond to the absence of AChR aggregates on each side of the original NMJs (see above).

The binding of ^{35}S-labeled agrin to the surface of the muscle fiber was specific. The injection of 10 times higher concentrations of unlabeled neural or muscle agrin 6 h before application of ^{35}S-labeled agrin markedly reduced the binding of ^{35}S-labeled neural or muscle agrin, respectively (Fig. 8 B, g and h). On the other hand, injection of 10 times higher concentrations of unlabeled neural agrin 6 h before application of ^{35}S-labeled muscle agrin did not reduce the binding of muscle agrin (Fig. 8 B, k).

Neural and Muscle Agrin Bind to Laminin

To examine whether the agrin binding to laminin could be responsible for homogenous distribution of recombinant agrin after application, muscles were injected with radioactive neural or muscle agrin (1 μM in 70 μl) and, 1 d later subjected to sequential extraction or immunoprecipitation, were followed by Western blot analysis. Muscle extracts and purified ^{35}S agrin were loaded onto 3-12% gradient gels under denaturing, reducing or non-denaturing, non-reducing conditions. Almost all ^{35}S agrin appeared in the fraction extracted with 5 μM EDTA and protease inhibitors in PBS, which is known to extract efficiently laminin (Paulsson et al., 1987). Under denaturing and reducing conditions, extracted and purified ^{35}S-labeled agrin migrated similarly but under nondenaturing, nonreducing conditions, extracted agrin failed to penetrate into the gel, suggesting that it was bound to other protein(s) (Fig. 9 A).

Recombinant neural and muscle agrin were immunoprecipitated from injected muscles and separated on 5% or 3–12% SDS-PAGE gradient gels. Silver staining revealed double bands of M_r ~200 and 400 kD, corresponding to the sizes of α, β, and γ chains of laminin, and agrin (Fig. 9 B). Western blot analysis of the immunoprecipitated complex using polyclonal antibody against α2-laminin detected a positive band at ~ 400 kD (Fig. 9 C). Together, these data indicate that both neural and muscle agrin bind to laminin in vivo.

Discussion

AChR Aggregation Induced by Recombinant Neural Agrin

In this work, we have applied purified recombinant agrin to skeletal muscles to study its effects in vivo in a more controlled way than done until now. We show that agrin
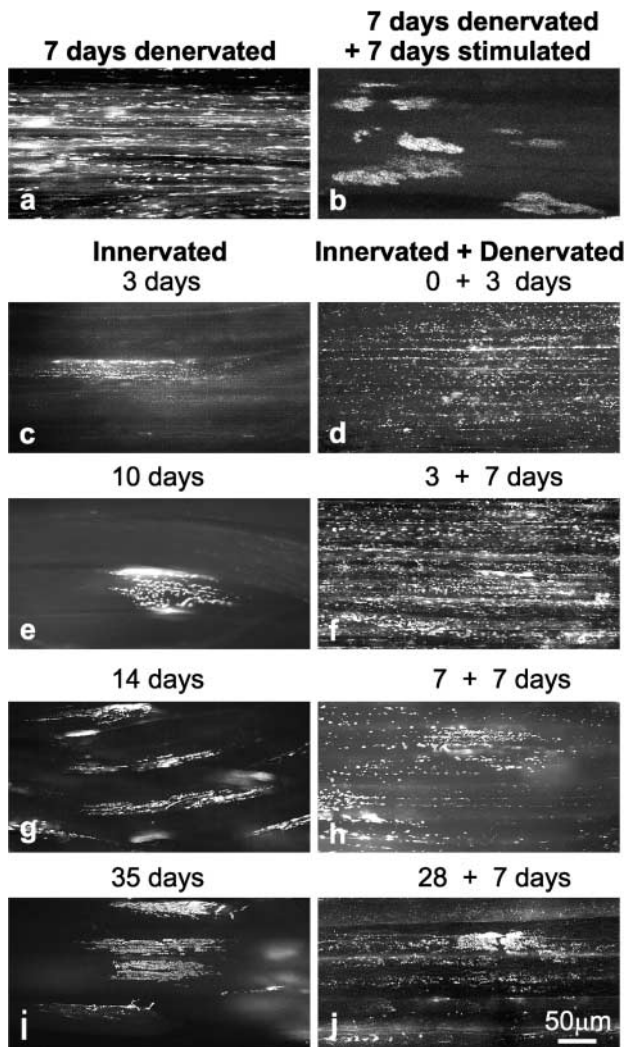
7 days denervated

7 days denervated + 7 days stimulated

Innervated 3 days

Innervated + Denervated 0 + 3 days

10 days

3 + 7 days

14 days

7 + 7 days

35 days

28 + 7 days

50 μm

Figure 7. Electrical muscle activity affects number, size, and distribution of neural agrin–induced AChR aggregates. 1 μM neural agrin was injected into SOL muscles that were immediately denervated (a, b, and d) or kept innervated (c and e–j). Muscles denervated for 7 d (a) were then electrically stimulated for additional 7 d (b). Some innervated muscles were denervated 0 (d), 3 (f), 7 (h), or 28 (j) d after the injection. At the indicated days after these treatments (3–35 d), the muscles were excised and treated with Rh-BuTx to label AChR aggregates as shown. Note the changes in number, size, and distribution of AChR aggregates that were caused by electrical stimulation of denervated muscles (compare a with b) and the similarity between aggregates in denervated stimulated (b) and innervated (c, e, g, and i) muscles. Also, note the appearance of a declining number of additional small AChR aggregates after denervating the innervated muscles ≤28 d after the injection of neural agrin (d, f, h, and j).

AChR–aggregating activities (EC_{50}) are ~3 nM in denervated and 30 nM in innervated muscle fibers, which are 100 and 1,000 times higher than reported for cultured myotubes (Gesemann et al., 1995) using the same chick agrin isoform. We bathed the SOL in solutions of neural agrin. When necessary, we added fresh solution of appropriate concentration to keep the muscle fully immersed during the 2 h of incubation and afterwards examined only surface fibers that had been in direct contact with the solu-

tion. Therefore, we think that agrin concentration was roughly maintained at stated values during treatment and that the higher EC_{50} in vivo may be related in part to differences in the composition of extracellular matrix, particularly to the amount of laminin known to bind agrin (Denzer et al., 1995, 1997; Kammerer et al., 1999), and in part to differences in responsiveness of embryonic and adult muscle cells to neural agrin.

The threshold concentration and EC_{50} for AChR aggregation by neural agrin was ~100 and ~10 times higher in innervated than in denervated muscles, respectively. Electrical muscle activity downregulates the expression of MuSK, which is a part of an agrin receptor and essential for AChR aggregation by neural agrin (DeChiara et al., 1996). The higher threshold in innervated muscles may therefore be related to a lower amount of MuSK along the innervated fibers. Muscles denervated at the time of injection displayed similar threshold concentration and EC_{50} as muscles denervated 7 d before the injection, consistent with the notion that denervation causes rapid upregulation of MuSK (Valenzuela et al., 1995), which can be then recruited into an agrin-induced scaffold. In innervated muscle fibers that normally do not express AChR ε-subunits in nonsynaptic regions (Witzemann et al., 1991, 1990), the AChR aggregates induced by neural agrin contained primarily ε-subunits. In contrast, in denervated muscle fibers, the aggregates were composed mainly of γ-subunit. Thus, in innervated fibers, AChR aggregation may depend on agrin-induced synthesis of synapse-specific proteins involving upregulation of MuSK (Meier et al., 1997; Jones et al., 1999), whereas in denervated fibers, aggregation of proteins already upregulated by denervation may be initially sufficient.

Individual AChR aggregates induced by high concentrations of neural agrin became smaller in size but more intensely labeled with Rh-BuTx. Weak Rh-BuTx staining often surrounded these aggregates, suggesting that AChRs translocated from larger to smaller aggregates. This reorganization was observed in predenervated, acutely denervated and innervated muscles, and may be related to agrin-induced organization of cytoskeletal proteins and colocalized AChRs (Bezakova and Lømo, 2001, page 1453, this issue). It did not depend on AChR subunit composition since denervated muscles containing primarily γ-subunit and innervated muscles containing mainly ε-subunit of AChR behaved similarly.

A single injection of neural agrin (1 μM) induced AChR aggregates that persisted ≥7 wk. During this period, a single injection of Rh-BuTx into denervated muscle labeled AChR aggregates that subsequently underwent changes in size and distribution along the fibers. Despite these changes, aggregates labeled by Rh-BuTx at a time when the AChRs contained γ- rather than ε-subunits, were still clearly visible 2 wk later. Furthermore, at this late time, newly inserted AChRs labeled by Fl-BuTx precisely colocalized with those labeled 2 wk earlier by Rh-BuTx (Fig. 2 B). Two conclusions may be drawn from these results. First, γ-subunit containing AChRs can be metabolically stabilized by neural agrin in agreement with our earlier finding that neural agrin alone can fully stabilize AChRs in a dose-dependent manner (Bezakova, G., I. Rabben, G. Fumagalli, and T. Lømo, submitted for publication). Sec-
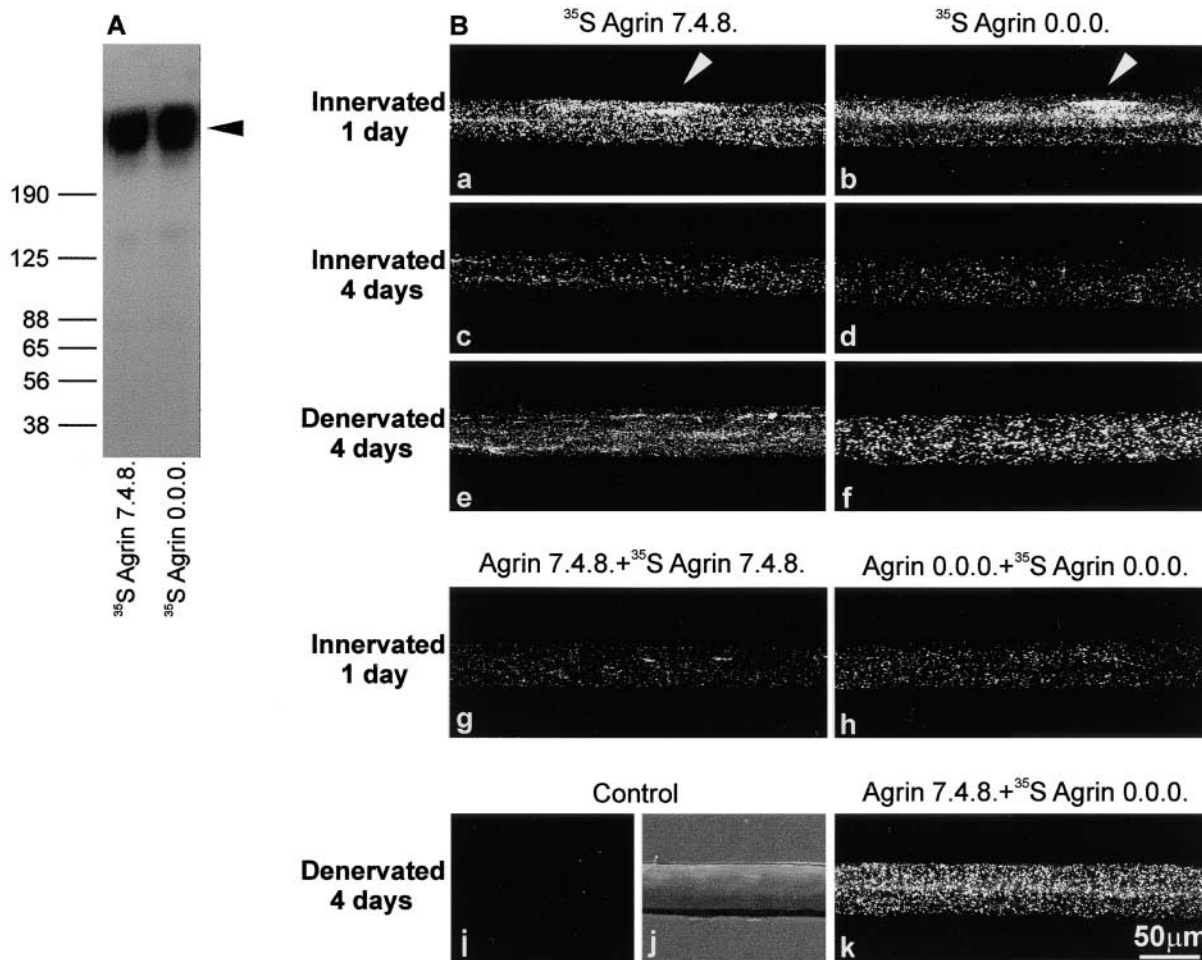
Figure 8. Binding of neural and muscle agrin to the surface of SOL muscle fibers. Radioactive (^{35}S) neural (isoform 7.4.8) and muscle (isoform 0.0.0) chick agrin were purified from stably transfected 293 HEK cells (see Materials and Methods) and separated by SDS-PAGE 3–12% gradient gel electrophoresis (A). 1 μM ^{35}S-labeled neural or muscle agrin was injected into SOL muscles, which were removed 1 or 4 d later for isolation of single fibers and subsequent autoradiography (B). Arrows in a and b, respectively, point to high density of bound neural and muscle agrin at a site in the middle of the fiber that probably corresponds to original NMJ. Note similar densities of neural and muscle agrin 4 d after injection in innervated (compare c with d) and denervated (compare e with f) fibers and lower densities in innervated (c and d) compared with denervated (e and f) fibers. Injection of 10 μM unlabeled agrin 6 h before injection of 1 μM radioactive agrin markedly reduced binding of the corresponding radioactive agrin (g and h). Fibers teased from muscles injected with PBS displayed essentially no grains (i and j, autoradiography and phase contrast, respectively). Injection of 10 μM unlabeled neural agrin did not reduce the binding of radioactive muscle agrin injected at 1 μM concentration 6 h later (k). The images show representative distribution of agrin after different treatments. Three muscles for each condition, and 10 randomly teased fibers from each muscle were examined.

ond, although, the aggregates labeled by Rh-BuTx underwent changes in size and distribution, they become stable in the sense that they determined the site of insertion of new AChRs. Presumably, this sort of stability is related to the agrin-induced organization of cytoskeletal proteins and colocalized AChR aggregates described elsewhere (Bezakova and Lømo, 2001, page 1453, this issue).

Binding of Injected Agrin to the Surface of Muscle Fibers

Neural Agrin. Neural agrin bound uniformly along the entire length of the muscle fibers, in contrast to the AChR aggregates it induced, which were nonuniformly distributed. In denervated muscles, large numbers of aggregates appeared along the fibers except in a region, ~0.5–0.8-mm long, on either side of the original NMJs. This region, as opposed to the rest of the fiber, is also refractory to ec-

topic NMJ formation by transplanted axons (Lømo, 1980). Since neural agrin bound as well in this region as elsewhere, the refractoriness cannot be attributed to surface changes that compromise agrin binding. Nor can it be attributed to lack of AChRs as their density is higher close to denervated NMJs than further away (Salpeter et al., 1988). Kues et al. (1995) provide evidence that nerve terminals at NMJs release a trophic signal, which in the continued presence of the nerve but independently of impulse activity down regulates the expression of certain genes (AChR γ-subunit, myogenin) in perisynaptic regions. The refractoriness addressed here, however, does not require the continued presence of the nerve since it persisted around the original NMJs after denervation. But it does require electrical muscle activity since it appears around developing ectopic NMJs only if the muscle is electrically
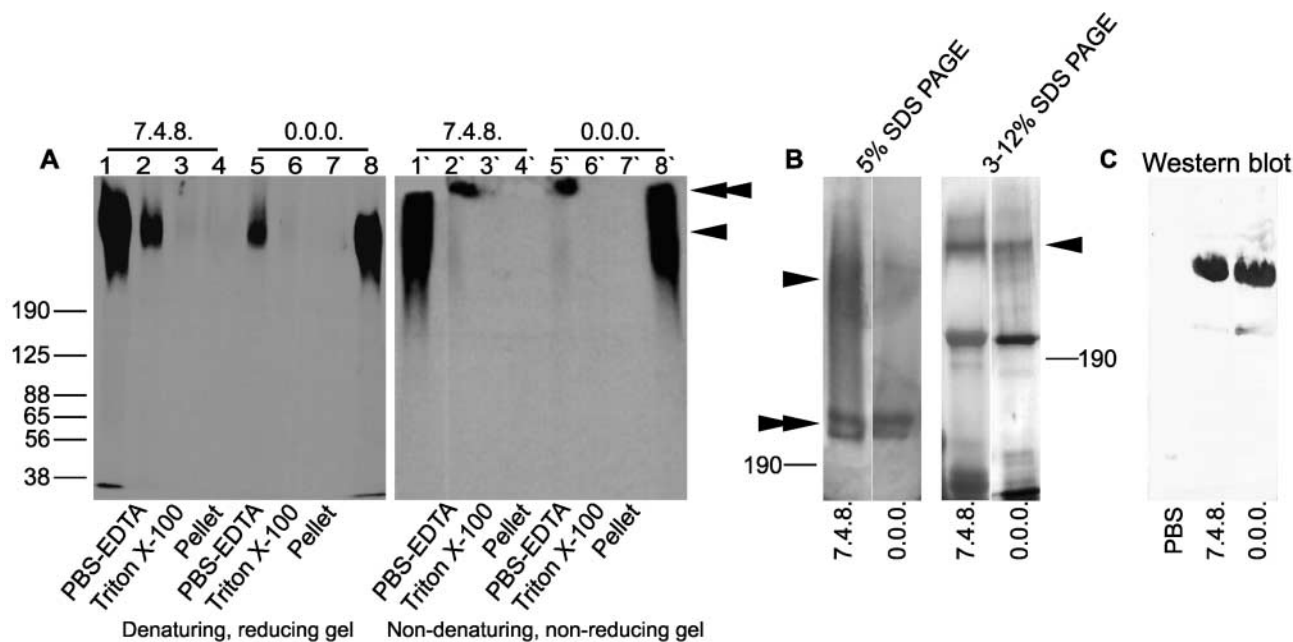
Figure 9. Agrin binds to laminin. SOL muscles were injected with 1 μM radioactively labeled neural or muscle agrin. 1 d later the muscles were excised, sequentially extracted, and analyzed by 3–12% SDS-PAGE electrophoresis under denaturing and reducing conditions (A, lanes 1–8) or nondenaturing and nonreducing conditions (A, lanes 1′–8′) followed by autoradiography. Lanes 1, 8, 1′, and 8′ represent the migration of purified radioactive neural and muscle agrin, respectively. Injected recombinant agrin was extracted from the muscle by PBS containing EDTA (lanes 2, 5, 2′, and 5′). The migration of extracted agrin was dependent on the conditions used to run the gel, indicating its binding to other protein(s). (B) SOL extracts were also immunoprecipitated with mAb 5B1 against agrin. Silver staining revealed the presence of bands having molecular mass ~400 and ~200 kD. Western blots of the immunoprecipitated complex and use of polyclonal antibody against α2-laminin confirmed the presence of α2-laminin (C). The molecular masses of standard proteins are indicated in kD.

active (Skorpen et al., 1999). In agreement with this observation, the AChR aggregates induced by neural agrin became very few and far apart in innervated electrically active as well as in denervated and electrically stimulated muscles. Together, these findings strengthen earlier indications that electrical muscle activity, as normally imposed by the nerve, plays an important role in regulating the number, size, and spatial distribution of the postsynaptic specializations induced by neural agrin (Mathiesen et al., 1999).

Bound agrin disappeared faster from extrajunctional regions of innervated electrically active fibers than from denervated electrically inactive fibers. Initially, the density of agrin binding was similar in innervated and denervated fibers. Thus, electrical activity apparently does not affect agrin binding as such but causes a more rapid removal of already bound agrin. However, also in innervated fibers, the effect of a single injection of neural agrin was long lasting since AChR aggregates persisted ≥7 wk (Fig. 2 A). In addition, new AChR aggregates appeared even when the muscle was denervated as long as 4 wk after agrin injection (Fig. 7 j).

Electrical muscle stimulation of denervated muscle removed not only most of the agrin-induced AChR aggregates (the losers) but also reduced agrin at the sites of losers and elsewhere, except at the few aggregates that survived (the winners). The mechanism underlying this activity-dependent removal of agrin from nonjunctional regions is unclear. Synaptic and extrasynaptic basal laminas are immunologically distinguishable and differentially regulated by electrical muscle activity (Sanes and Lawrence, 1983). The faster removal of bound agrin from nonsynaptic

regions in electrically active fibers may therefore be secondary to an effect of activity on the basal lamina. Recently, it has been shown that matrix metalloproteinase-3 (MMP3) localized at the NMJ but also in extrajunctional regions can selectively remove agrin from synaptic basal lamina (VanSaun and Werle, 2000). Furthermore, agrin contains nine folistatin domains that are related to Kazal protease inhibitors (Rupp et al., 1991). Depending on agrin binding to other proteins, these modules may acquire specific structural organization (Bork et al., 1996). It is therefore possible that the folistatin domains protect agrin from the degradation only at sites where agrin is part of a receptor complex that survives electrical muscle activity.

Muscle Agrin. Muscle agrin bound to the surface of innervated and denervated muscle fibers essentially as neural agrin with regard to density and distribution along the fibers. Muscle agrin, however, did not cause aggregation of AChRs. As was the case for neural agrin, nonradioactive muscle agrin significantly decreased the binding of subsequently applied radioactive muscle agrin, indicating that the binding in both cases was specific. In contrast, an excess of nonradioactive muscle agrin did not decrease subsequent binding of neural agrin nor did an excess of neural agrin decrease subsequent binding by muscle agrin, suggesting that muscle and neural agrin bind to different receptors or different parts of the same receptor.

Laminin 2. We provide evidence here that both muscle and neural agrin bind to laminin containing α2-chain in vivo. Agrin binding to laminin has been well characterized in vitro (Denzer et al., 1995, 1997; Kammerer et al., 1999).

Laminin isoforms 2 and 4 are predominant laminin isoforms of basal lamina and are expressed in developing muscle fibers (Chiu and Sanes, 1984; Sanes et al., 1990). Moreover, laminin-like immunoreactivity colocalizes with agrin-like immunoreactivity in chick embryo hind limb muscle in vivo and in vitro, and laminin as well as agrin are enriched in AChR clusters (Godfrey et al., 1988; Nitkin and Rothschild, 1990). In skeletal muscle, laminin also binds to integrin, particularly α7β1 integrin (von der Mark et al., 1991; Song et al., 1992) and induces colocalization of integrin and AChRs (Burkin et al., 1998). The recruitment of integrin into the AChR aggregates is further enhanced by the presence of agrin, and the response induced by both laminin and agrin can be inhibited by mAbs against α7 subunit of integrin. The integrin receptor associates with the cytoskeleton (Song et al., 1993) and is capable of signal transduction from the extracellular matrix (Clark and Brugge, 1995; Kwon et al., 2000). It is, thus, possible that integrin could be a component of the multisubunit receptor involved in agrin-induced synapse formation. Interestingly, in this work neural agrin induced the appearance of AChR aggregates predominantly near the myotendinous junction of innervated muscles, where the expression of α7β1 integrin is particularly pronounced (Mayer et al., 1997).

In vitro, agrin binds to both laminin and, in a Ca^{2+}-dependent manner, to α-dystroglycan (Gee et al., 1994; Denzer et al., 1997, Kammerer et al., 1999). We did not examine whether agrin also binds to α-dystroglycan in vivo because such binding is difficult to resolve in the presence of large amounts of laminin whose binding to α-dystroglycan is also Ca^{2+} dependent. Laminin may play a role in stabilizing and maintaining the postsynaptic apparatus (Denzer et al., 1997). Binding of neural agrin to laminin, and possibly to α-dystroglycan as well, may therefore have contributed to the long-lasting effect of a single injection of neural agrin that we observed.

Conclusion. We show that injected recombinant neural and muscle agrin bind to the surface of muscle fibers in vivo. Agrin binding involves laminin 2, is uniform along the fibers, and is regulated by muscle activity. Aggregation of AChRs by neural agrin is also muscle activity and dose dependent and characterized by higher EC_{50} in comparison to cultured myotubes. AChR aggregation does not appear in perisynaptic regions, although neural agrin initially binds as well in this region as elsewhere. A single application of neural agrin induces AChR aggregates that persist in the innervated and denervated muscles ≥7 wk. Finally, we show that a single application of purified recombinant agrin is a suitable method for studying important aspects of NMJ formation in vivo.

References

Bezakova, G., and T. Lømo. 2001. Muscle activity and muscle agrin regulate the organization of cytoskeletal proteins and attached acetylcholine esterase (AChR) aggregates in skeletal muscle fibers. *J. Cell Biol.* 153:1453–1463.

Bork, P., A.K. Downing, B. Kieffer, and I.D. Campbell. 1996. Structure and distribution of modules in extracellular proteins. *Q. Rev. Biophys.* 29:119–167.

Brenner, H.R., T. Lømo, and R. Williamson. 1987. Control of end-plate channel properties by neurotrophic effects and by muscle activity in rat. *J. Physiol.* 388:367–381.

Burkin, D.J., M. Gu, B.L. Hodges, J.T. Campanelli, and S.J. Kaufman. 1998. A functional role for specific spliced variants of the α7β1 integrin in acetylcholine receptor clustering. *J. Cell Biol.* 143:1067–1075.

Chiu, A.Y., and J.R. Sanes. 1984. Development of basal lamina in synaptic and extrasynaptic portions of embryonic rat muscle. *Dev. Biol.* 103:456–467.

Clark, E.A., and J.S. Brugge. 1995. Integrins and signal transduction pathways: the road taken. *Science.* 268:233–239.

Cohen, M.W., and E.W. Godfrey. 1992. Early appearance of and neuronal contribution to agrin-like molecules at embryonic frog nerve-muscle synapses formed in culture. *J. Neurosci.* 12:2982–2992.

Cohen, I., M. Rimer, T. Lømo, and U.J. McMahan. 1997. Agrin-induced postsynaptic apparatus in skeletal muscle fibers in vivo. *Mol. Cell. Neurosci.* 9:237–253.

DeChiara, T.M., D.C. Bowen, D.M. Valenzuela, M.V. Simmons, W.T. Poueymirou, S. Thomas, E. Kinetz, D.L. Compton, E. Rojas, J.S. Park, et al. 1996. The receptor tyrosine kinase MuSK is required for neuromuscular junction formation in vivo. *Cell.* 85:501–512.

Denzer, A.J., M. Gesemann, B. Schumacher, and M.A. Ruegg. 1995. An NH$_2$-terminal extension is required for the secretion of chick agrin and its binding to extracellular matrix. *J. Cell Biol.* 131:1547–1560.

Denzer, A.J., R. Brandenberger, M. Gesemann, M. Chiquet, and M.A. Ruegg. 1997. Agrin binds to the nerve–muscle basal lamina via laminin. *J. Cell Biol.* 137:671–683.

Gautam, M., P.G. Noakes, L. Moscoso, F. Rupp, R.H. Scheller, J.P. Merlie, and J.R. Sanes. 1996. Defective neuromuscular synaptogenesis in agrin-deficient mutant mice. *Cell.* 85:525–535.

Gee, S.H., F. Montanaro, M.H. Lindenbaum, and S. Carbonetto. 1994. Dystroglycan-a, a dystrophin-associated glycoprotein, is a functional agrin receptor. *Cell.* 77:675–686.

Gesemann, M., A.J. Denzer, and M.A. Ruegg. 1995. Acetylcholine receptor-aggregating activity of agrin isoforms and mapping of the active site. *J. Cell Biol.* 128:625–636.

Gesemann, M., V. Cavalli, A.J. Denzer, A. Brancaccio, B. Schumacher, and M.A. Ruegg. 1996. Alternative splicing of agrin alters its binding to heparin, dystroglycan, and the putative agrin receptor. *Neuron.* 16:755–767.

Glass, D.J., D.C. Bowen, T.N. Stitt, C. Radziejewski, J. Bruno, T.E. Ryan, D.R. Gies, S. Shah, K. Mattsson, S.J. Burden, P.S. DiStefano, D.M. Valenzuela, T.M. DeChiara, and G.D. Yancopoulos. 1996. Agrin acts via a MuSK receptor complex. *Cell.* 85:513–523.

Godfrey, E.W., R.E. Siebenlist, P.A. Wallskog, L.M. Walters, D.L. Bolender, and D.E. Yorde. 1988. Basal lamina components are concentrated in premuscle masses and at early acetylcholine receptor clusters in chick embryo hindlimb muscles. *Dev. Biol.* 130:471–486.

Gu, Y., P. Camacho, P. Gardner, and Z.W. Hall. 1991. Identification of two amino acid residues in the ε subunit that promote mammalian muscle acetylcholine receptor assembly in COS cells. *Neuron.* 6:879–887.

Hoch, W., M. Ferns, J.T. Campanelli, Z.W. Hall, and R.H. Scheller. 1993. Developmental regulation of highly active alternatively spliced forms of agrin. *Neuron.* 11:479–490.

Jones, G., A. Herczeg, M.A. Ruegg, M. Lichtsteiner, S. Kröger, and H.R. Brenner. 1996. Substrate-bound agrin induces expression of acetylcholine receptor ε-subunit gene in cultured mammalian muscle cells. *Proc. Natl. Acad. Sci. USA.* 93:5985–5990.

Jones, G., T. Meier, M. Lichtsteiner, V. Witzemann, B. Sakmann, and H.R. Brenner. 1997. Induction by agrin of ectopic and functional postsynaptic-like membrane in innervated muscle. *Proc. Natl. Acad. Sci. USA.* 94:2654–2659.

Jones, G., C. Moore, S. Hashemolhosseini, and H.R. Brenner. 1999. Constitutively active MuSK is clustered in the absence of agrin and induces ectopic postsynaptic-like membranes in skeletal muscle fibers. *J. Neurosci.* 19:3376–3383.

Kammerer, R.A., T. Schulthess, R. Landwehr, B. Schumacher, A. Lustig, P.D. Yurchenco, M.A. Ruegg, J. Engel, and A.J. Denzer. 1999. Interaction of agrin with laminin requires a coiled-coil conformation of the agrin-binding site within the laminin g1 chain. *EMBO J.* 18:6762–6770.

Kues, W.A., M.R. Brenner, B. Sakmann, and V. Witzemann. 1995. Local neurotrophic repression of gene transcripts encoding fetal AChRs at rat neuromuscular synapses. *J. Cell Biol.* 130:949–957.

Kwon, M.S., C.S. Park, K. Choi, J. Ahnn, J.I. Kim, S.H. Eom, S.J. Kaufman, and W.K. Song. 2000. Calreticulin couples calcium release and calcium influx in integrin-mediated calcium signaling. *Mol. Biol. Cell.* 11:1433–1443.

Laemmli, U.K. 1970. Cleavage of structural proteins during the assembly of the head of bacteriophage T4. *Nature.* 227:680–685.

Lømo, T. 1980. Requirements for the formation and maintenance of neuromuscular connections. *Curr. Top. Dev. Biol.* 16:253–281.

Lømo, T., and C.R. Slater. 1978. Control of acetylcholine sensitivity and syn-

apse formation by muscle activity. *J. Physiol*. 275:391–402.

Ma, E., R. Morgan, and E.W. Godfrey. 1994. Distribution of agrin mRNAs in the chick embryo nervous system. *J. Neurosci*. 14:2943–2952.

Magill-Solc, C., and U.J. McMahan. 1990. Synthesis and transport of agrin-like molecules in motor neurons. *J. Exp. Biol*. 153:1–10.

Magill-Solc, C., and U.J. McMahan. 1988. Motor neurons contain agrin-like molecules. *J. Cell Biol*. 107:1825–1833.

Mathiesen, I., M. Rimer, O. Ashtari, I. Cohen, U.J. McMahan, and T. Lømo. 1999. Regulation of the size and distribution of agrin-induced postsynaptic-like apparatus in adult skeletal muscle by electrical muscle activity. *Mol. Cell Neurosci*. 13:207–217.

Mayer, U., G. Saher, R. Fassler, A. Bornemann, F. Echtermeyer, H. von der Mark, N. Miosge, E. Poschl, and K. von der Mark. 1997. Absence of integrin α 7 causes a novel form of muscular dystrophy. *Nat. Genet*. 17:318–323.

McMahan, U.J. 1990. The agrin hypothesis. *Cold Spring Harb. Symp. Quant. Biol*. LV:407–418.

Megeath, L.J., and J.R. Fallon. 1998. Intracellular calcium regulates agrin-induced acetylcholine receptor clustering. *J. Neurosci*. 18:672–678.

Meier, T., D.M. Hauser, M. Chiquet, L. Landmann, M.A. Ruegg, and H.R. Brenner. 1997. Neural agrin induces ectopic postsynaptic specializations in innervated muscle fibers. *J. Neurosci*. 17:6534–6544.

Missias, A.C., G.C. Chu, B.J. Klocke, J.R. Sanes, and J.P. Merlie. 1996. Maturation of the acetylcholine receptor in skeletal muscle: regulation of the AChR γ-to-ϵ switch. *Dev. Biol*. 179:223–238.

Nastuk, M.A., E. Lieth, J.Y. Ma, C.A. Cardasis, E.B. Moynihan, B.A. McKechnie, and J.R. Fallon. 1991. The putative agrin receptor binds ligand in a calcium-dependent manner and aggregates during agrin-induced acetylcholine receptor clustering. *Neuron*. 7:807–818.

Nitkin, R.M., and T.C. Rothschild. 1990. Agrin-induced reorganization of extracellular matrix components on cultured myotubes: relationship to AChR aggregation. *J. Cell Biol*. 111:1161–1170.

Paulsson, M., M. Aumailley, R. Deutzmann, R. Timpl, K. Beck, and J. Engel. 1987. Laminin-nidogen complex. Extraction with chelating agents and structural characterization. *Eur. J. Biochem*. 166:11–19.

Reist, N.E., C. Magill, and U.J. McMahan. 1987. Agrin-like molecules at synaptic sites in normal, denervated, and damaged skeletal muscles. *J. Cell Biol*. 105:2457–2469.

Reist, N.E., M.J. Werle, and U.J. McMahan. 1992. Agrin released by motor neurons induces the aggregation of acetylcholine receptors at neuromuscular junctions. *Neuron*. 8:865–868.

Rimer, M., I. Mathiesen, T. Lømo, and U.J. McMahan. 1997. γ-AChR/ϵ-AChR switch at agrin-induced postsynaptic-like apparatus in skeletal muscle. *Mol. Cell. Neurosci*. 9:254–263.

Rotzler, S., and H.R. Brenner. 1990. Metabolic stabilization of acetylcholine receptors in vertebrate neuromuscular junction by muscle activity. *J. Cell Biol*. 111:655–661.

Ruegg, M.A., K.W. Tsim, S.E. Horton, S. Kröger, G. Escher, E.M. Gensch, and U.J. McMahan. 1992. The agrin gene codes for a family of basal lamina proteins that differ in function and distribution. *Neuron*. 8:691–699.

Rupp, F., D.G. Payan, C. Magill-Solc, D.M. Cowan, and R.H. Scheller. 1991. Structure and expression of a rat agrin. *Neuron*. 6:811–823.

Rupp, F., T. Ozcelik, M. Linial, K. Peterson, U. Francke, and R. Scheller. 1992. Structure and chromosomal localization of the mammalian agrin gene. *J. Neurosci*. 12:3535–3544.

Salpeter, M.M., and M. Azabo. 1976. An improved Kodak emulsion for use in high resolution electron microscope autoradiography. *J. Histochem. Cytochem*. 24:1204–1206.

Salpeter, M.M., M. Marchaterre, and R. Harris. 1988. Distribution of extrajunctional acetylcholine receptors on a vertebrate muscle: evaluated by using a scanning electron microscope autoradiographic procedure. *J. Cell Biol*. 106: 2087–2093.

Sanes, J.R., and J.C. Lawrence, Jr. 1983. Activity-dependent accumulation of basal lamina by cultured rat myotubes. *Dev. Biol*. 97:123–136.

Sanes, J.R., and J.W. Lichtman. 1999. Development of the vertebrate neuromuscular junction. *Annu. Rev. Neurosci*. 22:389–442.

Sanes, J.R., D.D. Hunter, T.L. Green, and J.P. Merlie. 1990. S-laminin. *Cold Spring Harb. Symp. Quant. Biol*. 55:419–430.

Sanes, J.R., E.D. Apel, M. Gautam, D. Glass, R.M. Grady, P.T. Martin, M.C. Nichol, and G.D. Yancopoulos. 1998. Agrin receptors at the skeletal neuromuscular junction. *Ann. NY Acad. Sci*. 841:1–13.

Skorpen, J., S. Lafond-Benestad, and T. Lømo. 1999. Regulation of the size and distribution of ectopic neuromuscular junctions in adult skeletal muscle by nerve-derived trophic factor and electrical muscle activity. *Mol. Cell Neurosci*. 13:192–206.

Smith, M.A., and D.K. O'Dowd. 1994. Cell-specific regulation of agrin RNA splicing in the chick ciliary ganglion. *Neuron*. 12:795–804.

Song, W.K., W. Wang, R.F. Foster, D.A. Bielser, and S.J. Kaufman. 1992. H36-α 7 is a novel integrin α chain that is developmentally regulated during skeletal myogenesis. *J. Cell Biol*. 117:643–657.

Song, W.K., W. Wang, H. Sato, D.A. Bielser, and S.J. Kaufman. 1993. Expression of α 7 integrin cytoplasmic domains during skeletal muscle development: alternate forms, conformational change, and homologies with serine/threonine kinases and tyrosine phosphatases. *J. Cell Sci*. 106:1139–1152.

Towbin, H., T. Staehelin, and J. Gordon. 1979. Electrophoretic transfer of proteins from polyacrylamide gels to nitrocellulose sheets: procedure and some applications. *Proc. Natl. Acad. Sci. USA*. 76:4350–4354.

Turney, S.G., S.M. Culican, and J.W. Lichtman. 1996. A quantitative fluorescence-imaging technique for studying acetylcholine receptor turnover at neuromuscular junctions in living animals. *J. Neurosci. Methods*. 64:199–208.

Valenzuela, D.M., T.N. Stitt, P.S. DiStefano, E. Rojas, K. Mattsson, D.L. Compton, L. Nunez, J.S. Park, J.L. Stark, D.R. Gies, et al. 1995. Receptor tyrosine kinase specific for the skeletal muscle lineage: expression in embryonic muscle, at the neuromuscular junction, and after injury. *Neuron*. 15: 573–584.

VanSaun, M., and M.J. Werle. 2000. Matrix metalloproteinase-3 removes agrin from synaptic basal lamina. *J. Neurobiol*. 43:140–149.

von der Mark, H., J. Durr, A. Sonnenberg, K. von der Mark, R. Deutzmann, and S.L. Goodman. 1991. Skeletal myoblasts utilize a novel β 1-series integrin and not α 6 β 1 for binding to the E8 and T8 fragments of laminin. *J. Biol. Chem*. 266:23593–23601.

Windisch, A., K. Gunderson, M.J. Szaboles, H. Gruber, and T. Lømo. 1998. Fast to slow transformation of denervated and electrically stimulated rat muscle. *J. Physiol*. 510:623–632.

Witzemann, V., E. Stein, B. Barg, T. Konno, M. Koenen, W. Kues, M. Criado, M. Hofmann, and B. Sakmann. 1990. Primary structure and functional expression of the α-, β-, γ-, δ- and ϵ-subunits of the acetylcholine receptor from rat muscle. *Eur. J. Biochem*. 194:437–448.

Witzemann, V., H.R. Brenner, and B. Sakmann. 1991. Neural factors regulate AChR subunit mRNAs at rat neuromuscular synapses. *J. Cell Biol*. 114:125–141.